Journal of Alloys and Compounds 502 (2010) 503–507

Contents lists available at ScienceDirect

Journal of Alloys and Compounds

journal homepage: www.elsevier.com/locate/jallcom

A study on 70 MPa metal hydride hydrogen compressor

Hui Li[a], Xinhua Wang[a,*], Zhaohui Dong[b], Lou Xu[a], Changpin Chen[a]

[a] *Department of Materials Science and Engineering, Zhejiang University, Hangzhou 310027, PR China*
[b] *Zhejiang Metallurgical Research Institute, Hangzhou 310017, PR China*

ARTICLE INFO

Article history:
Received 26 November 2009
Received in revised form 27 April 2010
Accepted 28 April 2010
Available online 5 May 2010

Keywords:
Metal hydrides
Hydrogen storage materials
Hydrogen compressor
High-pressure hydrogen

ABSTRACT

With the development of hydrogen storage technique using lightweight high-pressure hydrogen storage tank, high efficient hydrogen compression is of great interest. The objective of this study is to produce hydrogen with pressure of over 70 MPa by using a thermally driven hydride compressor. To reach this target, the hydrogen storage properties of La–Ce–Ca–Ni–Al family AB_5 type and Ti–Zr–Cr–Fe–V family AB_2 type multicomponent alloys have been investigated. $La_{0.35}Ce_{0.45}Ca_{0.2}Ni_{4.95}Al_{0.05}$ alloy was developed as the first stage hydrogen compression alloy, and $Ti_{0.8}Zr_{0.2}Cr_{0.95}Fe_{0.95}V_{0.1}$ as the second stage hydrogen compression alloy. With these two alloys, a double-stage compressor with hydrogen compression capacity of around 2000 L/cycle was designed and built, oil was used as the cooling and heat medium. When hot oil of 423 K is used as the heat source, product hydrogen with pressure of 74.5 MPa can be obtained, and the hydrogen flow rate of the compressor reaches 34.6 L/min.

1. Introduction

Hydrogen has been received much attention because it is a clean and widely available energy carrier. With the rapid development of hydrogen fuel cell vehicle (HFCV), hydrogen storage technique becomes more and more important. Recently, many famous vehicle companies adopt high-pressure (35 MPa) lightweight hydrogen storage vessel as hydrogen supplier for hydrogen fuel cell vehicle. In some developed countries, the working pressure of hydrogen storage tank increases to 70 MPa. With the development of high-pressure hydrogen storage technology, it is of interest to develop high efficient hydrogen compression technology.

The hydrogen desorption plateau pressure of a metal hydride varies with the temperature according to van't Hoff's equation. Based on this property, a metal hydride hydrogen compressor can be composed [1–9]. Hydride hydrogen compressor has been known for almost 40 years. In 1973, Vanmal [1] reported a hydride compressor for a hydrogen refrigerator, in which $LaNi_5$ is utilized to compress hydrogen from 4 to 45 atm. In 1980s, Nomura et al. [3] reported a hydrogen compressor using $LaNi_5$ as the energy conversion medium. It is able to desorb 360 L/min (NTP) of high-pressure (18–12 atm) hydrogen gas continuously in 3 min. Since then many research groups have been engaged in the area of hydride hydrogen compression. Silvaa [5] reported an industrial prototype of a hydrogen compressor based on FeTi metallic hydride technology, which desorbs the pressurized hydrogen of 10 MPa at 250 °C. The pilot sample of metal hydride hydrogen compressor was reported by Shmal'ko et al. [6]. The compressor consists of two two-stage compressing modules, in which $LaNi_{4.5}Mn_{0.5}$ and $LaNi_5$ are used as 'low temperature' and 'high temperature' hydride-forming intermetallides, respectively, and the pressure of output hydrogen reached 15 MPa. The American company Ergenics [10] has been supplying metal hydride hydrogen compressors for over twenty years. The reported six-stage hydride compressor can boost hydrogen pressure from atmospheric to 3000 psi (21 MPa) using energy from 85 °C hot water. Recently, Laurencelle et al. [11] reported a three-stage metal hydride hydrogen compressor which performs a thermal cycling of three AB_5 hydrogen storage alloys ($LaNi_{4.8}Sn_{0.2}$, $LaNi_5$ and $MmNi_{4.7}Al_{0.3}$) between 20 and 80 °C. The maximum hydrogen pressure produced by this three-stage metal hydride hydrogen compressor is around 22.61 atm. Cieslik et al. [12] developed a compressor model using $LaNi_{4.8}Sn_{0.2}$ (45 kg) and $LaNi_{4.25}Al_{0.75}$ (3.5 kg) alloys, which works between 310 and 450 K and the maximum hydrogen pressure reached 3.3 MPa. Popeneciu et al. [13] reported a three-stage hydrogen thermal compressor based on metal hydrides of $LaNi_{4.85}Al_{0.15}$, $LaNi_{4.9}Cu_{0.1}$ and $MmNi_{4.05}Fe_{0.95}$ alloys. The compressor works between 20 and 80 °C, and can raise the hydrogen pressure from 2 bars to 56 bars. In order to improve the efficiency of a hydrogen compression system, Kim et al. [14] uses porous metal hydride pellets of $LaNi_{5-x}Al_x$ to compose the compressor. Muthukumar et al. [15] tested a metal hydride hydrogen compressor using $MmNi_{4.6}Al_{0.4}$. When it works at 95 °C hot fluid temperature, the compressor can raise hydrogen from 5 bars to 43.8 bars. In our previous work [4,16–19], we have developed hydride hydrogen compressors with hydrogen pressure of 15–40 MPa.

---

[*] Corresponding author. Tel.: +86 571 8795 2716; fax: +86 571 8795 2716.
E-mail address: xinhwang@zju.edu.cn (X.H. Wang).

0925-8388/$ – see front matter © 2010 Elsevier B.V. All rights reserved.
doi:10.1016/j.jallcom.2010.04.206

Although hundreds of compositions of hydrogen storage alloys have been reported in literatures, these alloys were not studied for the purpose of hydride compression. The hydrogen storage alloys used in most cases of hydride compressor have not been optimized, $LaNi_5$, $La(NiAl)_5$, TiFe hydrogen storage alloys are generally selected, and the product hydrogen pressure of most of the reported hydride compressors is usually less than 15 MPa, which cannot meet the requirement of filling 40–70 MPa hydrogen storage tank.

In this paper, we report our results of a 70 MPa thermally driven hydride compressor, in which La–Ce–Ca–Ni–Al family AB_5 type alloy was developed as the first stage hydrogen compression alloy, and Ti–Zr–Cr–Fe–V family AB_2 type alloy as the second stage hydrogen compression alloy. When hot oil of 423 K is used as the heat source, hydrogen with pressure of 74.5 MPa can be produced.

2. Experimental details

The purity of the raw materials used in this study is 99.9% for La, Ce, Ni, and Cr, 99.5% for Ti, Zr, V, Al and Fe, and 98% for Ca. During alloy optimization, the alloys were prepared by induction levitation melting the constituent metals in a water-cooled copper crucible under argon atmosphere. In order to guarantee the homogeneity, the ingot was re-melted three times. Because the maximum melting capacity of our induction levitation melting furnace is around 100 g, the total amount of alloys for our designed compressor is around 27 kg, therefore, the alloys used to build the final compressor were prepared in an RF induction furnace under the protection of Ar instead of by induction levitation melting furnace. The *p*–*c*–*T* measurements show that there is no significant difference between the samples prepared by the two melting methods.

Structural analysis was carried out using a Rigaku D/max-3B X-ray diffractometer using Cu-Kα radiation at room temperature. The hydrogen storage properties of alloys were measured by using a homemade *p*–*c*–*T* apparatus. Samples were mechanically crushed into fine powder in air, and then introduced into a stainless steel reactor for measurements. Activation measurements were carried out at room temperature and under pressure of 6.0 MPa for AB_5 type alloys, and at 258 K and 30 MPa for AB_2 type alloys. After several hydrogen absorption/desorption cycles were carried out to ensure the samples were fully activated, *p*–*c*–*T* curves were then determined by the constant volume and pressure difference method. Cold oil (around 298 K) and hot oil (around 423 K) were used as the cooling and heating sources for hydrogen compression test. The pressure sensor (0–40 MPa) for *p*–*c*–*T* apparatus is LDN-500 type bought from Jiangmen Leader Information Technology Co. Ltd. (http://www.leadersensors.com), the pressure gauges for the compressors (0–60 MPa for the first stage compressor and 0–90 MPa for the second stage compressor) are CHY-2A type bought from Hunan Scientific Technology Co., Ltd. (http://www.yuhang.com.cn/zh-CN/index.html), and the data acquisition units for pressure and temperature are bought from Xiamen Yudian Automation Technology Co., Ltd. (http://www.yudian.com).

3. Results and discussion

The target pressure of product hydrogen is 70 MPa, if it is produced by a single stage metal hydride hydrogen compressor, the working temperature of the metal hydride hydrogen compressor (MHHC) will reach 200–300 °C. For the safety purpose of this study, we adopt oil as the cooling and heating media. It is better to control the working temperature of the hot oil below 180 °C. In order to meet thermal driving condition of metal hydride compressor, a double-stage compressor was designed and built to fulfill the target of 70 MPa pressure. With hot oil of around 150 °C, the first stage compressor converts hydrogen from 4–5 MPa to 35–40 MPa, and the second stage compressor then increases the pressure to over 70 MPa.

3.1. First stage hydrogen compression alloy

The objective of the first compressor is to compress hydrogen from 4–5 MPa to 35–40 MPa. In order to reach such a target under mild conditions, the alloy selected should have relatively high hydrogen absorption/desorption plateau pressure under ambient temperature. Because the favorable hydrogen storage properties of AB_5 type alloys, we tried to find an AB_5 type alloy as the first stage hydrogen compression alloy. Among the AB_5 type alloys, $LaNi_5$ has excellent hydrogen storage properties at room temperature, but its plateau pressure is too low. Our previous investigation [17–19] revealed that partial substitution of La with Ce and Ca in $La_{1-x-y}Ce_xCa_yNi_5$ system improves the activation properties as well as the plateau pressures, and the optimum Ca substitution content is 0.2–0.3. Additionally, partial substitution of Ni by Al can improve the hysteresis properties. Based on the above analysis, we designed and prepared $La_{0.35}Ce_{0.45}Ca_{0.2}Ni_{4.95}Al_{0.05}$ alloy. Fig. 1 shows the XRD pattern of the prepared alloy. The alloy mainly consists of $CaCu_5$ type structure. Fig. 2 shows the *p*–*c*–*T* curves of $La_{0.35}Ce_{0.45}Ca_{0.2}Ni_{4.95}Al_{0.05}$-H system. The alloy can be easily activated under 6.0 MPa at room temperature by several hydrogen absorption/desorption cycles. Its hydrogen storage capacity is 1.35 wt.%, hydrogen absorption plateau pressure at 298 K is around 1.91 MPa, hydrogen absorption/desorption hysteresis factor $\ln(P_a/P_d)$ is 0.4. The enthalpy of hydrogen desorption, ΔH_d, calculated from the middle plateau pressure in Fig. 2 according to van't Hoff equation is −29.5 kJ/molH$_2$. The theoretical hydrogen desorption plateau pressure at 423 K calculated according to van't Hoff equation is around 41.2 MPa. The above properties indicated that $La_{0.35}Ce_{0.45}Ca_{0.2}Ni_{4.95}Al_{0.05}$ is a suitable first stage compression alloy.

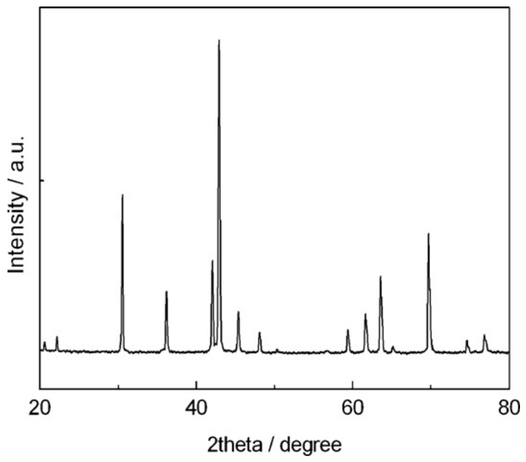

Fig. 1. XRD patterns of $La_{0.35}Ce_{0.45}Ca_{0.2}Ni_{4.95}Al_{0.05}$ alloy.

3.2. The second stage hydrogen compression alloy

Because the second hydrogen compression alloy should desorb hydrogen with high pressure of over 70 MPa when its hydride is heated to a suitable temperature, the optimum hydrogen storage alloy for this stage compressor should possess high plateau pressure at room temperature. The plateau pressure of Ti-based AB_2 type alloys can be regulated in a wider range, it is reasonable to develop an AB_2 type alloy as the second stage compression alloy for pairing with the developed AB_5 type alloys.

Ti–Cr–Fe AB_2 type alloys possess high plateau pressure, however, their hydrogen storage content is low and *p*–*c*–*T* plateau is slant. Our previous study indicates that partial substitution of Ti by Zr and partial substitution of Cr or Fe by V improve the plateau properties and increase the hydrogen storage content. Therefore, we designed and prepared $Ti_{0.8}Zr_{0.2}Cr_{1.9-x}Fe_xV_{0.1}$ ($x = 0.5, 0.95, 1.1, 1.2$) alloys. Fig. 3 shows the XRD patterns of the prepared alloys. All the alloys mainly consist of C14 Laves phase. Park [20] pointed out that the alloys will form C14 Laves phase when the averaged number of outer electrons (e/a) of AB_2 alloys is between 5.4 and 7.0. The e/a of the present alloys are 5.63, 5.93, 6.03 and 6.10. The results consist with Park's prediction. Moreover, the cell volume of the studied alloys decreases with increasing Fe content as shown

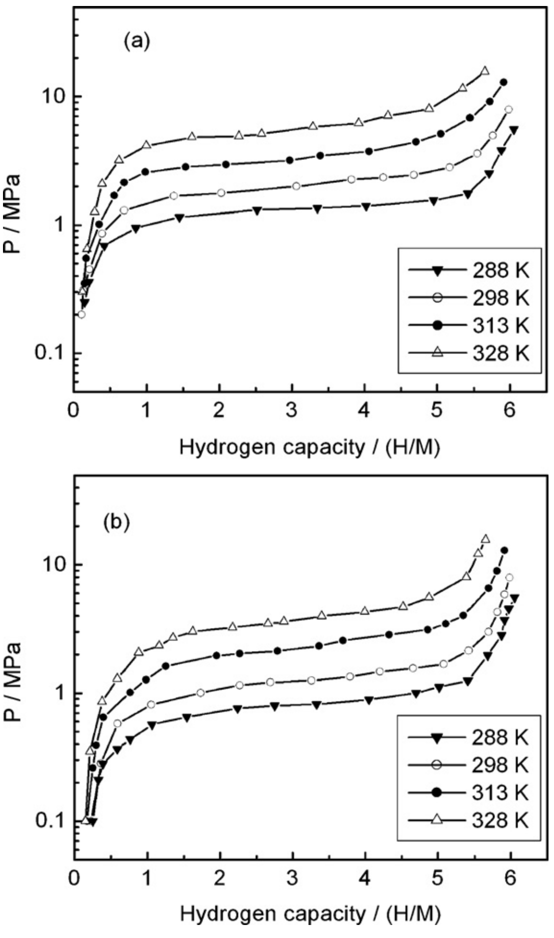

Fig. 2. *p*–*c*–*T* curves of $La_{0.35}Ce_{0.45}Ca_{0.2}Ni_{4.95}Al_{0.05}$-H system. (a) Absorption; (b) desorption.

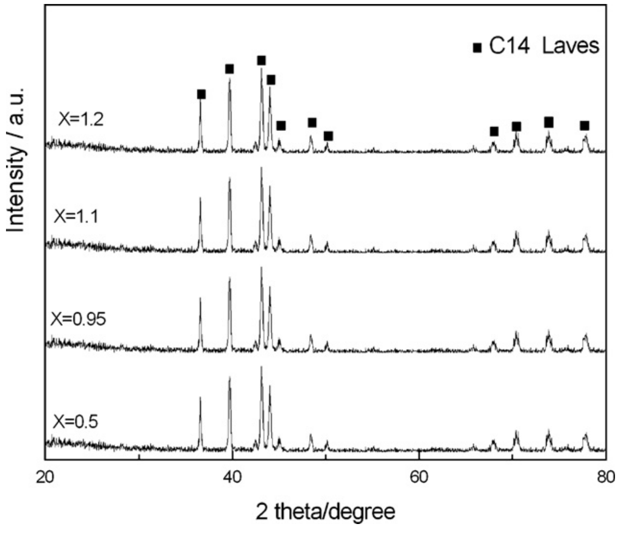

Fig. 3. XRD patterns of $Ti_{0.8}Zr_{0.2}Cr_{1.9-x}Fe_xV_{0.1}$ ($x = 0.5, 0.95, 1.1, 1.2$) alloys.

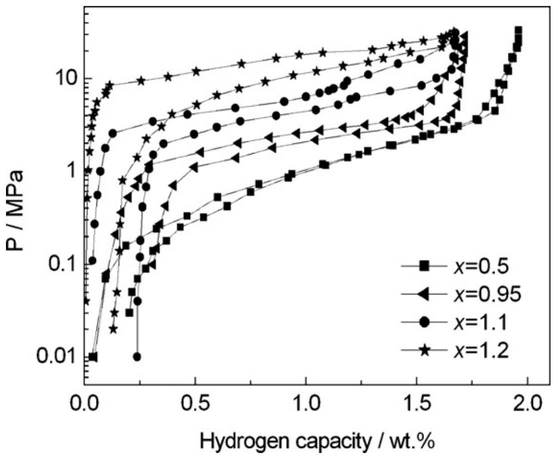

Fig. 4. *p*–*c*–*T* curves of $Ti_{0.8}Zr_{0.2}Cr_{1.9-x}Fe_xV_{0.1}$ ($x = 0.5, 0.95, 1.1, 1.2$) alloys at 258 K.

in Table 1, which is attributed to the larger radius of Cr than that of Fe.

Under the conditions of 30 MPa hydrogen pressure and 258 K, all alloys can be activated easily with several minutes of incubation time. As Fe content *x* increases from 0.5 to 1.2, the incubation time increases. We can conclude that addition of Fe makes activation of alloys more difficult.

Fig. 4 shows the *p*–*c*–*T* curves of $Ti_{0.8}Zr_{0.2}Cr_{1.9-x}Fe_xV_{0.1}$ at 258 K. Table 1 summarizes the main hydrogen storage properties of the alloys. From Fig. 4 and Table 1 it can be seen that as Fe content *x* increases, the hydrogen absorption and desorption plateau pressure increases and the hysteresis factor deceases, but the hydrogen storage capacity decreases. The increase of plateau pressure is due to the fact that the cell volume of the alloys decreases as Fe content increases. Among these alloys, $Ti_{0.8}Zr_{0.2}Cr_{1.4}Fe_{0.5}V_{0.1}$ has large hydrogen storage capacity and small hysteresis factor, however, its *p*–*c*–*T* plateau is relatively slant. Moreover, its plateau pressure is low for using as the second stage hydrogen compression alloy. With consideration of both the plateau characteristics and the matching properties with $La_{0.35}Ce_{0.45}Ca_{0.2}Ni_{4.95}Al_{0.05}$ alloy, $Ti_{0.8}Zr_{0.2}Cr_{0.95}Fe_{0.95}V_{0.1}$ is suitable for the second stage compression alloy.

Fig. 5 shows the *p*–*c*–*T* curves of $Ti_{0.8}Zr_{0.2}Cr_{0.95}Fe_{0.95}V_{0.1}$ alloy over wide rages of temperature and pressure. Its absorption/desorption plateau pressures at 298 K are 8.9 and 7.3 MPa, respectively. The enthalpy of hydrogen desorption, ΔH_d, calculated from the middle plateau pressure in Fig. 5 according to van't Hoff equation is around −20.5 kJ/molH$_2$. The theoretical hydrogen desorption plateau pressure at 423 K calculated according to van't Hoff equation is around 84.5 MPa.

3.3. Hydrogen compression properties of the double-stage compressor

With $La_{0.35}Ce_{0.45}Ca_{0.2}Ni_{4.95}Al_{0.05}$ as the first stage hydrogen compression alloy and $Ti_{0.8}Zr_{0.2}Cr_{0.95}Fe_{0.95}V_{0.1}$ as the second stage hydrogen compression alloy, a double-stage hydride hydrogen compressor was designed and built. 18 kg AB_5 type alloy and 9 kg AB_2 type alloy were used for the first stage and second stage

Table 1
Properties of $Ti_{0.8}Zr_{0.2}Cr_{1.9-x}Fe_xV_{0.1}$ alloys at 258 K.

Alloys	Hydrogen capacity (wt.%)	P_a (MPa)	P_d (MPa)	Hysteresis factor ($\ln(P_a/P_d)$)	*a* (Å^3)	*c* (Å^3)	Cell volume (Å^3)
$Ti_{0.8}Zr_{0.2}Cr_{1.4}Fe_{0.5}V_{0.1}$	1.96	1.13	1.04	0.08	4.95	8.07	171.2
$Ti_{0.8}Zr_{0.2}Cr_{0.95}Fe_{0.95}V_{0.1}$	1.72	2.45	2.02	0.19	4.89	8.02	166.3
$Ti_{0.8}Zr_{0.2}Cr_{0.8}Fe_{1.1}V_{0.1}$	1.68	5.40	3.97	0.31	4.88	8.03	165.6
$Ti_{0.8}Zr_{0.2}Cr_{0.7}Fe_{1.2}V_{0.1}$	1.67	16.53	10.14	0.49	4.85	8.03	163.6

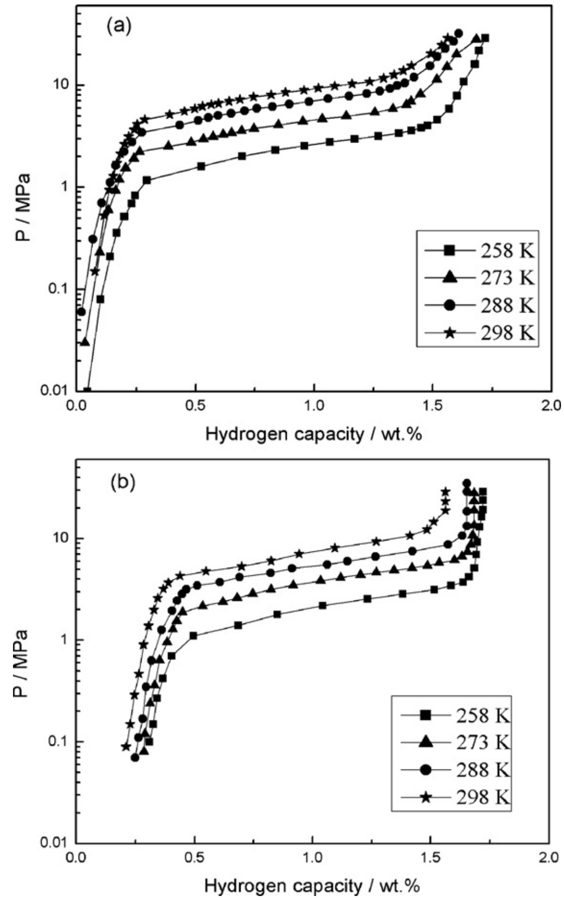

Fig. 5. *p*–*c*–*T* curves of $Ti_{0.8}Zr_{0.2}Cr_{0.95}Fe_{0.95}V_{0.1}$-H system. (a) Absorption; (b) desorption.

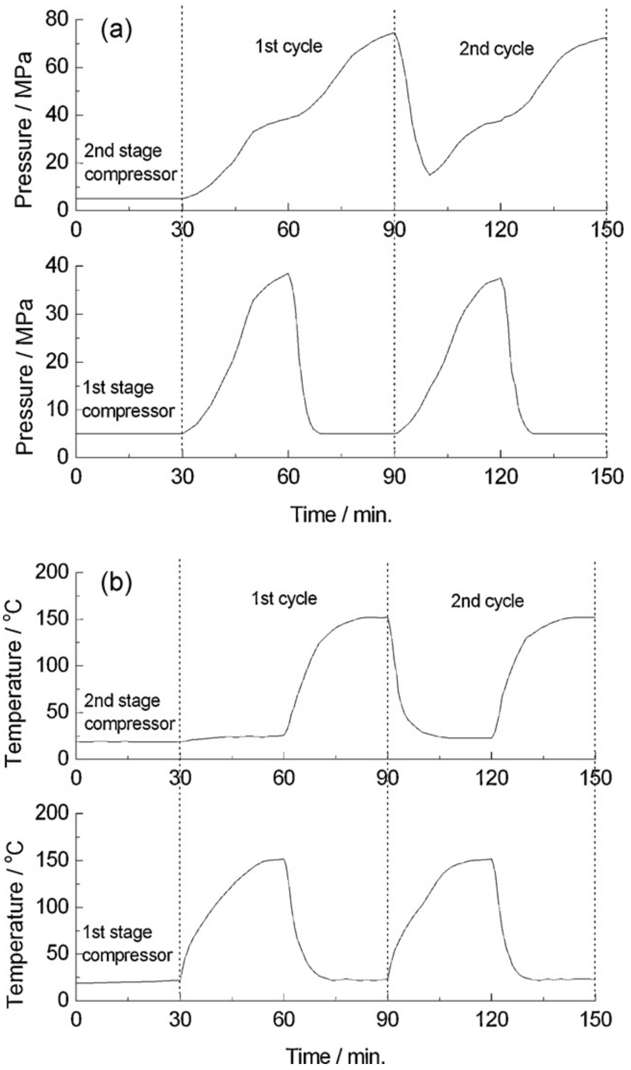

Fig. 7. Compression performance of the double-stage compressor. (a) Pressure–time curves; (b) Temperature–time curves.

compressors, respectively. For safety purpose, oil was used as the cooling and heating medium. The first stage compressor was composed of 14 steel tubes with 38 mm outer diameter and 5 mm wall thickness, and 2 electrical heating rods were set into the parallel of the tubes as the auxiliary heater. The second stage compressor was composed of 8 steel tubes with 32 mm outer diameter and 8 mm wall thickness, and an electrical heating rod was set into the parallel of the tubes as the auxiliary heater.

The target hydrogen compression capacity is 2000 L/cycle. To improve the compression efficiency of the system, the hydrogen capacity of the first stage compressor was designed to be 2 times of that of the second stage compressor. Namely, one for the first stage is more than 2000 L hydrogen and the other for the second stage is more than 1000 L hydrogen. Fig. 6 shows the schematic diagram of the double-stage compressor. The compression performance of the double-stage compressor is shown in Fig. 7. At first, the first stage compressor is circulated with cold oil to absorb hydrogen under around 5.0 MPa hydrogen pressure, then it is circulated with

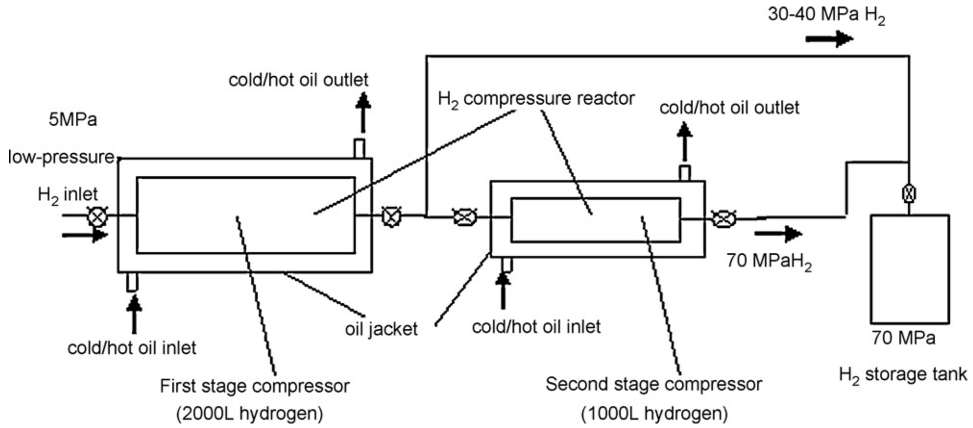

Fig. 6. Schematic diagram of the double-stage compressor.

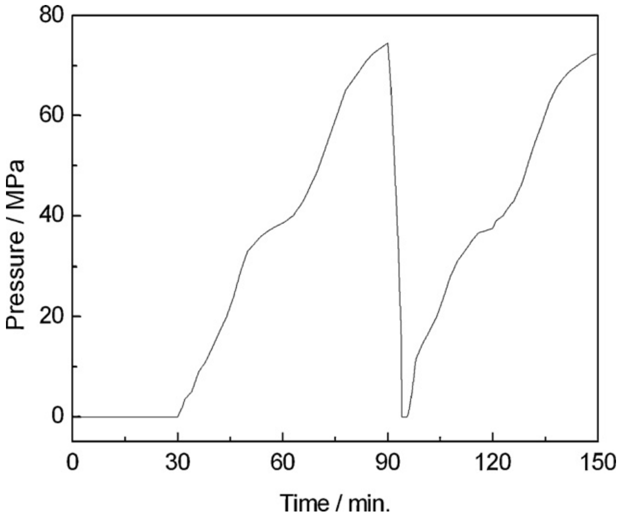

Fig. 8. Variation of pressure of hydrogen storage tank with time during compression process.

hot oil (around 423 K) and the inner heaters were used to maintain the oil temperature at the later stage of hydrogen desorption. At the first half cycle of the compression process, more than 2080 L (estimated from final volume of hydrogen filled into the hydrogen storage tank) hydrogen with pressure of 38.5 MPa can be produced by the first stage compressor. Around 1075 L hydrogen is supplied to the hydrogen storage tank (with inner volume of 2.85 L) directly, and the other part of hydrogen is absorbed by the second stage compression alloy (in this time, the second stage compressor is circulated with cold oil). It can be seen from Fig. 7 that there is a time hysteresis between the temperature variation and pressure variation. This is because the measured temperature is that of the oil instead of the hydride bed. The final hydrogen pressure achieved by the compressor is lower than the theoretically calculated hydrogen pressure from the hydrogen storage alloy, this can be ascribed to the fact that there exists dead volume in the hydride compressor bed and there also exists temperature difference between hot oil and the hydride bed. At the second half cycle of the compression process, hot oil of around 423 K is circulated into the second stage compressor (the inner heaters were also used to maintain the oil temperature at the later stage of hydrogen desorption) and cold oil is circulated into the first stage compressor. In this half cycle of compression process, 1005 L hydrogen with pressure of around 74.5 MPa is produced and filled into the hydrogen storage tank. Fig. 8 shows the variation of pressure of the hydrogen storage tank with time during compression process. The total time used for a full cycle is 60 min, so the hydrogen flow rate of the compressor is around 34.6 L/min. The cycling stability of the hydrogen storage alloy pair will be studied further.

4. Conclusions

Hydrogen storage properties of La–Ce–Ca–Ni–Al and Ti–Zr–Cr–Fe–V alloys have been studied for the application of hydrogen compression. $La_{0.35}Ce_{0.45}Ca_{0.2}Ni_{4.95}Al_{0.05}$ and $Ti_{0.8}Zr_{0.2}Cr_{0.95}Fe_{0.95}V_{0.1}$ alloys have satisfactory hydrogen storage characteristics and are suitable for the first stage and the second stage hydrogen compression alloys. With the developed alloys, a 70 MPa double-stage metal hydride hydrogen compressor with hydrogen compression capacity of around 2000 L/cycle has been designed and built with oil as the cooling/heating medium. When oil with temperature of 423 K was used as the heat source and hydrogen with pressure of 5 MPa as the feed gas, product hydrogen with pressure of over 70 MPa can be produced, and the hydrogen flow rate of the compressor reaches 34.6 L/min.

Acknowledgments

This work was supported by the foundation of Hi-tech Research and Development Program of China (No. 2006AA05Z129) and National Basic Research Program of China (Nos. 2007CB209706 and 2010CB631304).

References

[1] H.H. Vanmal, Chemie Ingenur Technik 45 (1973) 80–83.
[2] G. Sandrock, S. Suda, L. Schlabach, in: L. Schlabach (Ed.), Hydrogen in Intermetallic Compounds (II), Springer-Verlag, Berlin, 1992, pp. 197–258.
[3] K. Nomura, E. Akiba, S. Ono, J. Less-Common Met. 89 (1983) 551–558.
[4] Q.D. Wang, C.P. Chen, Y.Q. Lei, J. Alloys Compd. 253–254 (1997) 629–635.
[5] E.P.D. Silvaa, Int. J. Hydrogen Energy 18 (1993) 307–311.
[6] Y.F. Shmal'ko, A.I. Ivanovsky, M.V. Lototsky, V.I. Kolosov, D.V. Volosnikov, Int. J. Hydrogen Energy 24 (1999) 645–648.
[7] Z. Dehouche, N. Grimard, F. Laurencelle, J. Goyette, T.K. Bose, J Alloys Compd. 399 (2005) 224–236.
[8] A.I. Ivanovsky, V.I. Kolosov, M.V. Lototsky, V.V. Solovey, Y.F. Shmalko, Int. J. Hydrogen Energy 21 (1996) 1053–1057.
[9] P. Muthukumar, M.P. Maiya, S.S. Murthy, Int. J. Hydrogen Energy 27 (2002) 1083–1088.
[10] http://www.ergenics.com/page19.htm.
[11] F. Laurencelle, Z. Dehouche1, F. Morin, J. Goyette, J. Alloys Compd. 475 (2009) 810–816.
[12] J. Cieslik, P. Kula, S.M. Filipek, J. Alloys Compd. 480 (2009) 612–616.
[13] G. Popeneciu, V. Almasan, I. Coldea, D. Lupu, I. Misan, O. Ardelean, 182, J. Phys.: Conf. Ser. (2009) 012053, doi:10.1088/1742-6596/182/1/012053.
[14] J.K. Kim, I.S. Park, K.J. Kim, K. Gawlik, Int. J. Hydrogen Energy 33 (2008) 870–877.
[15] P. Muthukumar, M.P. Maiya, S.S. Murthy, Int. J. Hydrogen Energy 33 (2008) 463–469.
[16] C.P. Chen, Z. Ye, J. Wu, Q.D. Wang, Z. Phys. Chem. Neue Folge Bd 183 (1994) 251–258.
[17] X.H. Wang, R.G. Chen, Y. Zhang, C.P. Chen, Q.D. Wang, J. Alloys Compd. 420 (2006) 322–325.
[18] X.H. Wang, Y.Y. Bei, X.C. Song, G.H. Fang, S.Q. Li, C.P. Chen, Q.D. Wang, Int. J. Hydrogen Energy 32 (2007) 4011–4015.
[19] X.H. Wang, R.G. Chen, Y. Zhang, C.P. Chen, Q.D. Wang, Mater. Lett. 61 (2007) 1011–1014.
[20] J.G. Park, H.Y. Jang, S.C. Han, P.S. Lee, J.Y. Lee, J. Alloys Compd. 325 (2001) 293–298.